Simulation of Printer Nozzle for 3D Printing TNT/HMX Based Melt-Cast Explosive

Huzeng Zong
University of Science and Technology
Qilun Cong
University of Science and Technology
Tengyue Zhang
China Research and Development Academy of Machinery Equipment
Yanjun Hao
The third army agency office stationed in Taiyuan
Lei Xiao
National Special Superfine Powder Engineering Technology Research Center
Gazi Hao
National Special Superfine Powder Engineering Technology Research Center
Guangpu Zhang
National Special Superfine Powder Engineering Technology Research Center
Hu Guo
National Special Superfine Powder Engineering Technology Research Center
Yubing Hu
National Special Superfine Powder Engineering Technology Research Center
We Jiang (superfine_jw@126.com)
NJUST: Nanjing University of Science and Technology

Research Article

Keywords: 3D printing, TNT/HMX, FLUENT, Numerical simulation

Posted Date: June 11th, 2021

DOI: https://doi.org/10.21203/rs.3.rs-579750/v1

Abstract

Fused deposition modelling (FDM) has been one of the most widely used rapid prototyping (RP) technologies, which has been attracted increasing attentions in the world. However, existing literatures about energetic material flow inside the 3D printer nozzle are sparse. For plunger 3D printer, we summarized the experimental and related literatures, finding that viscosity, temperature, outlet velocity, pressure, and nozzle diameter are the main factors to affect the flow state in the nozzle. Based on the actual printer nozzle structure, in this paper, a finite element model was established by SOLIDWORKS software firstly, meanwhile, the flow channel model of the nozzle was extracted and simplified. Secondly, the factors influencing the printing results were researched and analysed. In the end, numerical simulation on velocity field and temperature field was carried out by FLUENT software. Moreover, the printing test of HMX/TNT was also carried out by using EAM-D-1 3D printer. The printed sample shows that 3D printing is more satisfactory than conventional melt-casting ways to prepare high viscocity and unconventional structure explosives

1. Introduction

3D printing has become commonplace for the manufacturing of objects with unusual geometries, and recent developments that enabled printing of multiple materials indicate that the technology can potentially offer a much wider design space beyond unusual shaping [1]. This is a work of making three-dimensional solid objects from digital files [2]. Compared to conventional manufacturing methods, 3D products can be created by acquired data or structures built in computer - aided design (CAD) software and reduce waste while reaching satisfactory geometric accuracy, thus, 3D printing has the advantage of higher quality, greater efficiency and reduce maintenance cost. 3D printing has found industrial applications in the automotive and aerospace industries for printing prototypes of car and airplane parts, and in the architectural world for printing structural models [3]. According to the state of materials, 3D printing can be divided into many types, such as stereolithography (SL) [4], Polyjet [5] fused deposition modeling (FDM) [6], laminated object manufacturing (LOM) [7], selective laser sintering (SLS) [8], laminated engineered net shaping (LENS) [9], Prometal [10], and so on.

FDM, as a kind of rapid prototyping technology, is one of the most widely used methods for rapid prototyping in the world and developed by Scott Cump of Stratasys. Low price, high speed and convenience of the process are the main benefits of FDM. The physical process of FDM method was a thermoplastic polymer is used to print layers of materials. The filament is heated at the nozzle to reach a molten or semi-liquid state and then extruded on the platform or on top of previously printed layers. The direction in which the head and platform are free to move depends on 3D printer type. In this study, the head moves on X-Y plane and deposits materials according to the geometry of the currently printed layer. After finishing a layer, the platform holding the part moves vertically in the Z direction to begin depositing a new layer on top of the previous one [11]. The thermoplasticity of the polymer filament is an essential property for this method, which allows the filaments to fuse together during printing and then to solidify [illegible] ntage of FDM is that it can be used to create

objects fabricated from multiple material types by printing and subsequently changing the print material, which enables more producer control over device fabrication for experimental use. Besides conventional materials such as PC [13], polystyrene (PS) [14], ABS [15], FDM can also be used to print 3D models by using metal [16], ceramics [17] and biomaterials [18]. FDM 3D printing technology can be applied in many fields, including energetic materials.

Melt cast explosives are used in mortars, grenades, artillery shells, warheads, and antipersonnel mines. 2,4,6-trinitrotoluene (TNT) based melt cast high explosive (HE) compositions occupy a premier position as fillings for warheads and projectiles due to extensive production facilities all over the globe, despite their limitations and the emergence of cast cured HE compositions [19]. An ideal melt-cast explosive or its formulations should have the following properties: (1) melting point 70–120℃, (2) low vapor pressure, (3) no shrinking and cracking on cooling, (4) no separation from the shell or casing, (5) high density and good energetic performance [20]. FDM 3D printing technology has been employed to fabricate melt-cast explosive. Previous researcher used an independently developed melt-cast explosive 3D printing principal prototype to prepare TNT/HMX based melt-cast explosives. The results show that 3D printing melt-cast explosives have more compacting internal structures with the density of 1.65 g/cm^3, the compressive strength of 5.56 MPa, and the detonation velocity of 7143 m/s [21]. Using this method can effectively avoid the generation of the shrinkage cavity and avert the internal porosity in the process of extrusion charge. In addition, He et al. prepared a gradient structured HMX/Al composite by using 3D printing technology, which can control the burning rate by change the component ratio [22]. In a word, FDM provides an innovative and reliable manufacturing method for explosive and can be regarded as one of the satisfactory ways to fabricate next-generation explosives with higher safety and better performance.

2. Materials And Method

High quality grade TNT and HMX with a purity of 99.9% were obtained from the Gansu Yin'guang chemical Industry group company limited, HMX conformed to the quality requirements of Chinese Military Standards (GJB) and its average particle size is between 120 ~ 160 μm. HLG-50 ball mill was researched and designed by National special superfine powder engineering research center of China. Malvern Mastersizer 2000 particle analyzer was used to measure the particle sizes of HMX after grinding. K6-MPC-NR Huber oil bath was used to provide heat for melting and maintaining temperature of molten TNT. Brookfield Digital Viscometer was used for measurement of viscosity of the TNT/HMX melts. EAM-D-1 3D printer was designed by Nanjing University of Science and Technology.

2.1 Preparation of ultra-fine HMX particles

Two materials were selected for this study, 2,4,6-trinitrotoluence (TNT) and octahdro-1,3,5,7-tetra-nitro-1,3,5,7-tetrazocine (HMX). TNT is a nitroaromatic explosive while HMX is classified as nitroamine [23]. TNT has stability in molten condition for most high explosive melt-cast due to its low melting temperature (80.6 ℃), good stability in molten condition for relatively long periods, high decomposition

temperature (240 ℃). However, TNT is less powerful, thus, other energetic compounds like HMX is incorporated into TNT to increase the efficiency of the composition [24].

The dispersion liquid was prepared in a ratio of 10:3:1 of ionized water, ethanol and isobutanol, then fully stirred and mixed with the raw particles HMX to prepare the suspension slurry. HLG-50 ball mill was used to grind the suspended slurry [25]. The grinding medium adopts 0.38 mm zirconia beads, and the grinding rate was set to 1200 rpm. By controlling the grinding time and beads filling ratio, HMX ultrafine particles with good dispersibility could be obtained after freeze-drying. After grinding, the slurry was freeze-dried, and the particle size was measured by the Malvern Mastersizer 2000 particle analyzer. The particle size distribution, shown in Fig. 1, is critical for enabling a smooth fluid inside nozzle. HMX particles with an average size of 1 μm, 6 μm, 13 μm, and 20 μm were selected. HMX particles were applied to TNT-based melt-cast explosives.

2.3 Effect of HMX content on viscosity

The particle size and its component ratio have been widely accepted as the vital factors affecting the viscosity of melts. The mixture of TNT/HMX was placed in the Huber oil bath at 95 ℃ and prepared to melt. During this time, continuous stirring and ultrasonic vibration are performed to ensure uniform mixing and remove air bubbles suspended in the molten explosives. Brookfield Digital Viscometer, Model DV-I was used to measure the viscosity of the melts. The 3D model of rotor is shown in Fig. 2.

Viscosity of various TNT/HMX compositions was measured at 95 ℃, shown in Fig. 3. Figure 3 infers that with the increasing content of HMX in TNT melt, viscosity increases accordingly. For a molten explosive with the same viscosity, the larger the particle size, the higher the maximum solid content. Because at the same solid content, the smaller particle size leads to larger number of particles contained, which reduces the average distance between particles. A relatively strong network structure is formed between particles, and the force required to break this structure increases, so the shear stress increases and viscosity increases. Besides, as the number of particles increases, the total effective volume of the particles increases, which can be attributed to the surface adsorption effect. A film was formed on surface, which makes the effective volume larger than the real volume, increasing the displacement resistance. Based on previous viscosity data, we used viscosity of 7500, 10000, 15000, 20000, 25000 mPa•s for the following simulations.

2.4 Simulation of squeeze injection pressure on flow state

The plunger 3D printer extrudes the energetic material from the nozzle by changing the pressure, so the change of the extrusion pressure has a significant impact on the printing effect. Adjusting the extrusion pressure to achieve the best printing effect is also the most convenient and commonly used method. Previous research has shown that the nozzle's suitable pressure can be obtained by simulation. Yao et al detailed the influence of direct writing pressure on ink flow process [26]. Aiman Sukindar et al using Finite Element Analysis (FEA) observed the pressure drop along the liquefier with different nozzle diameter [27]. Proper pressure plays an important role in printing process, combined with actual situation, 80, 90, 100,

een inlet pressure and outlet velocity of nozzle.

2.5 Simulation of nozzle diameter and melting temperature on flow state

Another critical element that has a high impact on the 3D printing process is the nozzle diameter. The nozzle diameter has a direct relationship with the outlet velocity, especially its flowability [28]. The nozzle with too large diameter will lead to difficult in forming, while with too small diameter may cause nozzle clogging. In our approach, we used different nozzle diameters ranging from 0.1mm to 0.7mm, this work was done to determine which diameter of nozzle is optimal for printing.

A great deal of fundamental research relevant to FDM processes has been performed since FDM became recognized as the most commercialized 3D printing process. The study of printing parameters on characteristics of the final products is a crucial topic to improve quality [29]. In this paper, the FDM uses TNT/HMX as raw material and heated to above the melting point of TNT and then dispensed on the plate layer-by-layer to produce the desired 3D structure. Thus, temperature is also important in printing process. According to the characteristics of TNT based explosives, we set the fluid temperature to 100 ℃ and observe the temperature decreasing along the flow channel.

3 Results And Discussion

3.1 Simplified model of nozzle

In order to simulate the temperature distribution of the nozzle shell during printing, the 3D model of the nozzle was designed in SolidWorks software according to actual measured size, the initial geometry of the object was constructed and meshed, the total length of nozzle was 14.4 mm, the diameter of inlet was 4 mm, and that of outlet was 0.58 mm. In addition, to simplify the process and improve accuracy, the external structure of nozzle was omitted. As shown in Fig. 4 (a) and4 (b).

The flow channel model of nozzle established by SolidWorks software to simulate changes in pressure and velocity of the internal flow field, as shown in Fig. 4 (c) and 4 (d). The model would be imported into ICEM CFD software. The inlet, outlet, and wall all defined in ANSYS Mesh component system. The finite element model would be imported into FLUENT software to carry out fluid analysis.

3.2. Simulation analysis of velocity

3.2.1 Effect of viscosity on velocity

The meshed flow channel model was imported into FLUENT software. The inlet pressure was set to 100 kPa and kept unchanged, meanwhile, the fluid viscosities of 7500 mPa·s, 10000 mPa·s, 15000 mPa·s, 20000 mPa·s and 25000 mPa·s were selected to represent the changes of melt-cast explosive in the flow channel. The velocity distribution in the flow channel was obtained, and the velocity contour at 25000 mPa•s is shown in Fig. 5. The velocity of fluid is low on the top and changes sharply where the nozzle [illegible]r to the periphery. According to the results of

speed distribution, it shows that all velocity distribution diagrams only differ in numerical values. In order to save space, only Fig. 5 is presented here. In addition, it can be noticed from Fig. 5 that the red part has the highest speed, which also represent the printing speed, so we take this flow velocity for further analyses.

The effect of viscosity on velocity was measured at 100 kPa pressure and data obtained are presented in Fig. 6. The velocity of the fluid decreases in a nonlinear relation with the increasing fluid viscosity, meanwhile, the slope of the curve also decreases. The trend of increase in viscosity with decrease of velocity can be attributed to the friction of wall. The expression of the fitting curve is as follows:

$$y = 69.5831x^{-0.9835} R^2 = 0.999$$

3.2.2 Effect of pressure on velocity

During printing process, energetic materials are deposited layer by layer. The improvement of item quality can be implemented by proper parameter setting, among those parameters, extrusion pressure is particularly important. In this paper, the relationship between extrusion pressure and flow rate was simulated. The melt-cast explosive viscosity was set to 15000 mPa·s, and the extrusion pressure was set to 80, 90, 100, 110 and 120 kPa respectively. The expression of the fitting curve is as follows:

$$y = 0.04769x + 0.0762 R^2 = 0.999$$

It can be seen from the Fig. 7 that as pressure increases, the maximum velocity of fluid in nozzle increases. In addition, a certain slope is obtained and there is a clearly linear relationship between the pressure (80–120 kPa) and velocity, which shows that pressure is a very important parameter for adjustment of print quality.

3.2.3 Effect of nozzle diameter on velocity

In order to investigate the effect of nozzle diameter on velocity, we set the pressure to 100kPa and the viscosity to 15000 mPa·s. Velocity of fluid was measured at seven different nozzle diameters (0.1, 0.2, 0.3, 0.4, 0.5, 0.6 and 0.7 mm). The function of nozzle diameter and velocity is shown in Fig. 8. It is clear that as nozzle diameter increases, the velocity increases accordingly. The expression of the fitting curve is as follows:

$$y = 8.3516x^{1.9635} R^2 = 0.999$$

3.3 Simulation analysis of temperature

3.3.1 The temperature distribution of flow channel

In order to model the heat transfer of fluid, the temperature distribution of nozzle's channel was simulated. The fluid viscosity was set to 15000 mPa·s, and the inlet velocity of fluid was set to 40 mm/s, [Loading [MathJax]/jax/output/CommonHTML/fonts/TeX/fontdata.js] ty of nozzle was structural steel.

As shown in Fig. 9, the inlet and outlet temperatures do not change significantly, but at the bend of the flow channel, due to narrowing of flow channel suddenly, which results in the reduction of the temperature. The difference between the highest temperature and the lowest temperature is 2.3 ℃. The simulation can be applied to check the actual working conditions.

3.3.2 The temperature distribution of nozzle

The nozzle was heated by a constant heating tube and take the top surface of nozzle as heating face. Once the heat transfer reaches a dynamic equilibrium, there is no heat exchange occurs with the outside, and the internal temperature remains constant. The steady-state thermal module was selected to simulate the temperature distribution of nozzle. The material of nozzle is structural steel.

It can be seen from the Fig. 10 that temperature decreases from top to bottom, about 3.4 ℃ difference between maximum temperature and minimum temperature, as the temperature distribution of the flow channel above. According to the simulation results, it illustrates that the nozzle with this structure can effectively avoid the blockage of the material due to the decreasing temperature before extrusion, which can provide theoretical support for selection of nozzle configuration and heating temperature. In any case, the minimum temperature of nozzle should be higher than melt point of melt-cast explosive.

As shown in Fig. 11, the nozzle's temperature gradually decreases from top to bottom and changes rapidly between point 1 and 2. Because in this position the nozzle diameter is larger than other position and the area contact with air get bigger, which causes the temperature drop faster than other positions. However, it can be noticed that all the temperatures are higher than the melting point of TNT.

3.4 3D printing HMX/TNT based explosives

Based on the previous basic research, HMX particle size between 1–15 μm were was fabricated on a bi-directional mill. The raw HMX and milled HMX as shown in Fig. 12. The raw HMX is prismatic and milled HMX is plate shaped. and the loading of TNT and HMX both restricted to 50% by weight, the nozzle diameter was 6 mm.

Figure 13 shows the printer is printing a cylinder (φ20×20). OM (OLMPUS BX53) and SEM (Phenom G2 Pro) were used to investigate the surface structure and morphology of products. Detailed informations are shown in Fig. 14.

Figure 14 shows flow chart of 3D printing HMX/TNT based explosives. As can be seen from the upper left corner, the products were prepared layer by layer. From the optical micrograph of Fig. 14 (a), the grooves can be found clearly between layer and layer, and the surface is smooth without scratchers and defects. Figure 14 (b) shows the SEM images of products (front view) almost every layer was divided into two parts. The bottom of every layer is tightly filled but at the top part exist many small holes. Because of during the printing process, the slurry will gradually solidify after being extruded from the nozzle, and the top parts solidfy faster than bottom due to contact with the air. Moreover, the bottom parts can be influenced by the extrusion pressure from nozzle and the gravity from the slurry itself, which makes the

bottom parts more tightly and compact than top parts. Just as the diagram on the top right. When the slurry layer extuded from the nozzle, the new layer will contact with the previous one. The new layer will sank and flatten due to the gravity and extrusion force. Moreover, the new layer will transfer heat to around when it begin solidiy, which can cause the precious layers to melt and solidify again. Figure 14 (c) shown that there is no obvious hole inside the grain, which proved 3D printing is more satisfactory than conventional melt-casting ways to prepare high viscocity and unconventional structure explosives.

Figure 15 presented the XRD pattern of HMX/TNT explosives prepared by melt cast and 3D printing, the sharp characteristic peak of HMX at 2θ = 14.7°, 16.1°, 20.4°, 23.0°, 31.9°, TNT at 2θ = 12.6°, 20.9°, 23.1° all can be found in melt casted and 3D printed products, which indicated that the raw materials exist in these two different preparation methods, and that the crystal forms of the HMX and TNT were not influenced by the melting process.

4 Conclusion

According to the existing literatures and researches [30–32], commonly additive manufacturing methods for energetic materials are mainly include inkjet printing method and fused deposition modelling method, and most of the researchers focus on solid rocket propellants. Although there are few reports on the 3D printing of melt-cast explosives, the studies above have shown that FDM has certain technical advantages in terms of quality and shaped structure for the preparation of melt-cast explosives. Moreover, the used methods can only simulate the situation where the fluid viscosity does not change, and the influence of wall roughness on fluid flow is ignored. The particles may precipitate during the actual printing process, which may cause nozzle blockage. In addition, according to the current common simulation methods, CFD coupled with DEM (Discrete Element Method) method may be a better way to simulate the coordinated movement of particles and fluid. This work can provide some theoretical and practical support for 3D printing energetic materials.

Declarations

Acknowledgements

The machines, devices, and tools used in this work are the properties of the National Special Superfine Powder Engineering Research Center of China.

Funding

This work was financially supported by the National Natural Science Foundation of China (No. 21805139 and 51706105), the Natural Science Foundation of Jiangsu Province (BK20170846), the Qing Lan Project, a project funded by the Priority Academic Program Development of Jiangsu Higher Education Institutions (PAPD), and Basic Product Innovation Technology Research Project of Explosives.

Availability of data and material

All authors affirm that this manuscript is an honest, accurate, and transparent account of the study being reported; that no important aspects of the study have been omitted; and that any discrepancies from the study as planned (and, if relevant, registered) have been explained.

Code availability

The datasets generated during and/or analyzed during the current study are available from the corresponding author on reasonable request.

Conflict of interest

The authors declare no competing interests.

Ethics approval

The submitted work is original and it not has been published elsewhere in any form or language.

Consent to participate

This research did not involve using of living beings (humans or animals) or organisms or anything vegetable species nor voluntary or involuntary participation in activities that cause detrimental or defamatory on humans in all experimental activities.

Consent for publication

Not applicable

References

1. Kokkinis D, Schaffner M, Studart AR (2015) Multimaterial magnetically assisted 3D printing of composite materials. Nat Commun 6: https://doi.org/10.1038/ncomms9643
2. Goodrich PJ, Sharifi F, Hashemi N (2015) Rapid prototyping of microchannels with surface patterns for fabrication of polymer fibers. RSC Adv 5:71203–71209. https://doi.org/10.1039/c5ra15154f
3. Gross BC, Erkal JL, Lockwood SY et al (2014) Evaluation of 3D printing and its potential impact on biotechnology and the chemical sciences. Anal Chem 86:3240–3253. https://doi.org/10.1021/ac403397r
4. Lee SJ, Nowicki M, Harris B, Zhang LG (2017) Fabrication of a Highly Aligned Neural Scaffold via a Table Top Stereolithography 3D Printing and Electrospinning. Tissue Eng - Part A 23:491–502. https://doi.org/10.1089/ten.tea.2016.0353
5. Meisel NA, Elliott AM, Williams CB (2015) A procedure for creating actuated joints via embedding shape memory alloys in PolyJet 3D printing. J Intell Mater Syst Struct 26:1498–1512. https://doi.org/10.1177/1045389X14544144

6. Melocchi A, Parietti F, Loreti G et al (2015) 3D printing by fused deposition modeling (FDM) of a swellable/erodible capsular device for oral pulsatile release of drugs. J Drug Deliv Sci Technol 30:360–367. https://doi.org/10.1016/j.jddst.2015.07.016
7. Zhang Y, He X, Du S, Zhang J (2001) Al2O3 ceramics preparation by LOM (laminated object manufacturing). Int J Adv Manuf Technol 17:531–534. https://doi.org/10.1007/s001700170154
8. Fina F, Goyanes A, Gaisford S, Basit AW (2017) Selective laser sintering (SLS) 3D printing of medicines. Int J Pharm 529:285–293. https://doi.org/10.1016/j.ijpharm.2017.06.082
9. Durejko T, Zietala M, Polkowski W, Czujko T (2014) Thin wall tubes with Fe3Al/SS316L graded structure obtained by using laser engineered net shaping technology. Mater Des 63:766–774. https://doi.org/10.1016/j.matdes.2014.07.011
10. Wong KV, Hernandez A (2012) A Review of Additive Manufacturing. ISRN Mech Eng 2012:1–10. https://doi.org/10.5402/2012/208760
11. Dudek P (2013) FDM 3D printing technology in manufacturing composite elements. Arch Metall Mater 58:1415–1418. https://doi.org/10.2478/amm-2013-0186
12. Ngo TD, Kashani A, Imbalzano G et al (2018) Additive manufacturing (3D printing): A review of materials, methods, applications and challenges. Compos Part B Eng 143:172–196. https://doi.org/10.1016/j.compositesb.2018.02.012
13. Mohamed OA, Masood SH, Bhowmik JL (2017) Experimental investigation of time-dependent mechanical properties of PC-ABS prototypes processed by FDM additive manufacturing process. Mater Lett 193:58–62. https://doi.org/10.1016/j.matlet.2017.01.104
14. Rymansaib Z, Iravani P, Emslie E et al (2016) All-Polystyrene 3D-Printed Electrochemical Device with Embedded Carbon Nanofiber-Graphite-Polystyrene Composite Conductor. Electroanalysis 28:1517–1523. https://doi.org/10.1002/elan.201600017
15. Dawoud M, Taha I, Ebeid SJ (2016) Mechanical behaviour of ABS: An experimental study using FDM and injection moulding techniques. J Manuf Process 21:39–45. https://doi.org/10.1016/j.jmapro.2015.11.002
16. Garg HK, Singh R (2017) Modelling the Peak Elongation of Nylon6 and Fe Powder Based Composite Wire for FDM Feedstock Filament. J Inst Eng Ser C 98:567–573. https://doi.org/10.1007/s40032-016-0250-0
17. Vorndran E, Klarner M, Klammert U et al (2008) 3D powder printing of β-tricalcium phosphate ceramics using different strategies. Adv Eng Mater 10:67–71. https://doi.org/10.1002/adem.200800179
18. Chia HN, Wu BM (2015) Recent advances in 3D printing of biomaterials. J Biol Eng 9:1–14. https://doi.org/10.1186/s13036-015-0001-4
19. Mishra VS, Vadali SR, Garg RK et al (2013) Studies on FOX-7 based melt cast high explosive formulations. Cent Eur J Energ Mater 10:569–580
20. Ravi P, Badgujar DM, Gore GM et al (2011) Review on melt cast explosives. Propellants Explos

201100047

21. Lei X, Wang Q, Li W (2018) Preparation and Performances of Nano-HMX and TNT Melt-cast Explosives Based on 3D Printing Technology. ACTA ARMAMENTAR II 39(7):1292–1298. doi:10.3969/j.issn.1000-1093.2018.07.006
22. He Q, Wang J, Mao Y et al (2021) Fabrication of gradient structured HMX/Al and its combustion performance. Combust Flame 226:222–228. https://doi.org/10.1016/j.combustflame.2020.12.003
23. Lynch JC, Brannon JM, Delfino JJ (2002) Dissolution rates of three high explosive compounds: TNT, RDX, and HMX. Chemosphere 47:725–734. https://doi.org/10.1016/S0045-6535(02)00035-8
24. An C, Wang J, Xu W, Li F (2010) Preparation and properties of HMX coated with a composite of TNT/energetic material. Propellants Explos Pyrotech 35:365–372. https://doi.org/10.1002/prep.200900060
25. Chen T, Zhang Y, Guo S, feng et al (2019) Preparation and property of CL-20/BAMO-THF energetic nanocomposites. Def Technol 15:306–312. https://doi.org/10.1016/j.dt.2018.08.013
26. Yilong Y, Jing W, Lizhi W (2016) Jet Flow Simulation of CL-20 Energetic Ink. Explosive Materials 45(4): 14–21. https: 10.3969/j.issn.1001-8352.2016.04.003
27. Sukindar NA, Ariffin MKA, Hang Tuah Baharudin BT et al (2016) Analyzing the effect of nozzle diameter in fused deposition modeling for extruding polylactic acid using open source 3D printing. J Teknol 78:7–15. https://doi.org/10.11113/jt.v78.6265
28. Malaeb Z, Hachem H, Tourbah A et al (2015) 3D Concrete Printing: Machine and Mix Design. Int J Civ Eng Technol 6:14–22
29. Hwang S, Reyes EI, Moon K et al (2015) Thermo-mechanical Characterization of Metal/Polymer Composite Filaments and Printing Parameter Study for Fused Deposition Modeling in the 3D Printing Process. J Electron Mater 44:771–777. https://doi.org/10.1007/s11664-014-3425-6
30. Chandru RA, Balasubramanian N, Oommen C, Raghunandan BN (2018) Additive manufacturing of solid rocket propellant grains. J Propuls Power 34:1090–1093. https://doi.org/10.2514/1.B36734
31. McClain MS, Gunduz IE, Son SF (2019) Additive manufacturing of ammonium perchlorate composite propellant with high solids loadings. Proc Combust Inst 37:3135–3142. https://doi.org/10.1016/j.proci.2018.05.052
32. Murray AK, Isik T, Ortalan V et al (2017) Two-component additive manufacturing of nanothermite structures via reactive inkjet printing. J Appl Phys 122:1–6. https://doi.org/10.1063/1.4999800

Figures

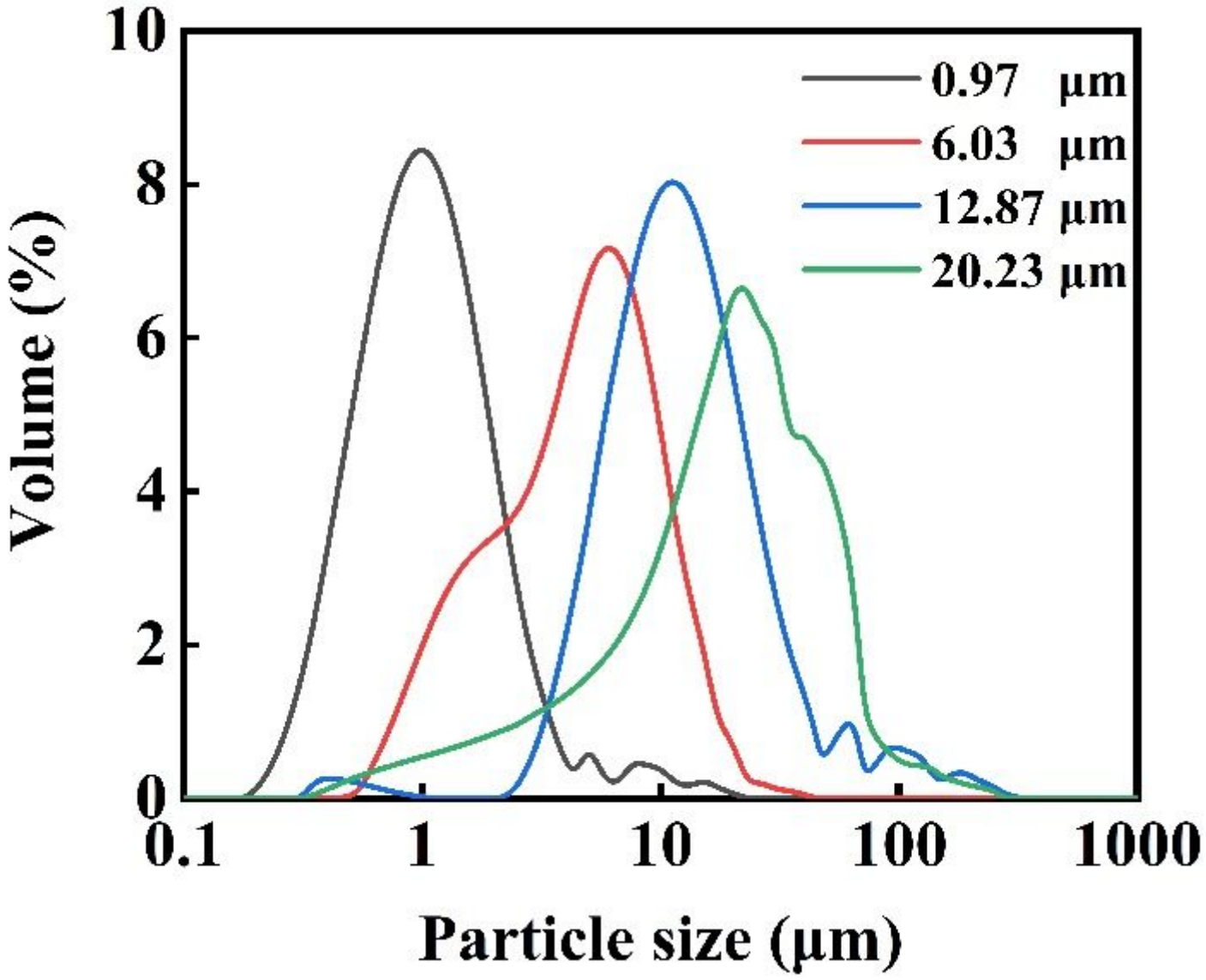

Figure 1

The particle size distribution of HMX.

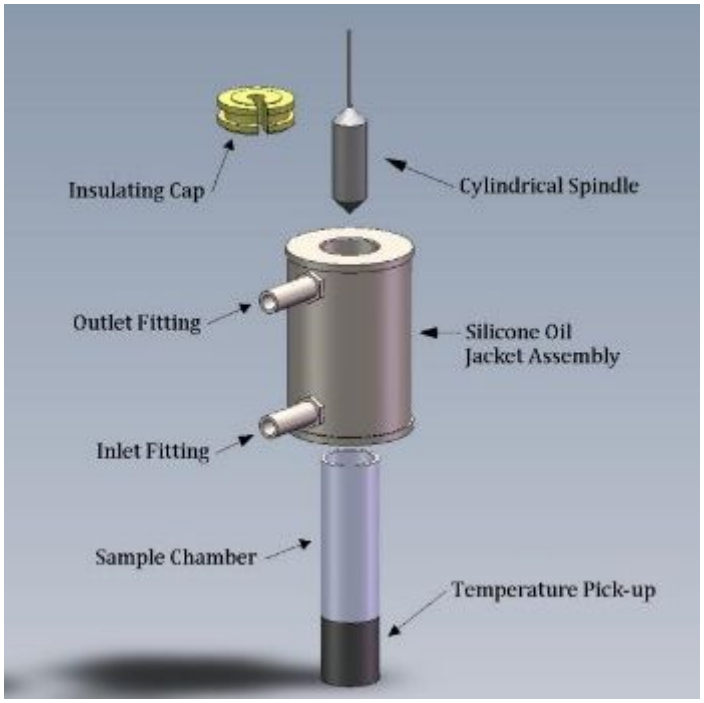

Figure 2

3D model of the cone-plate rotor.

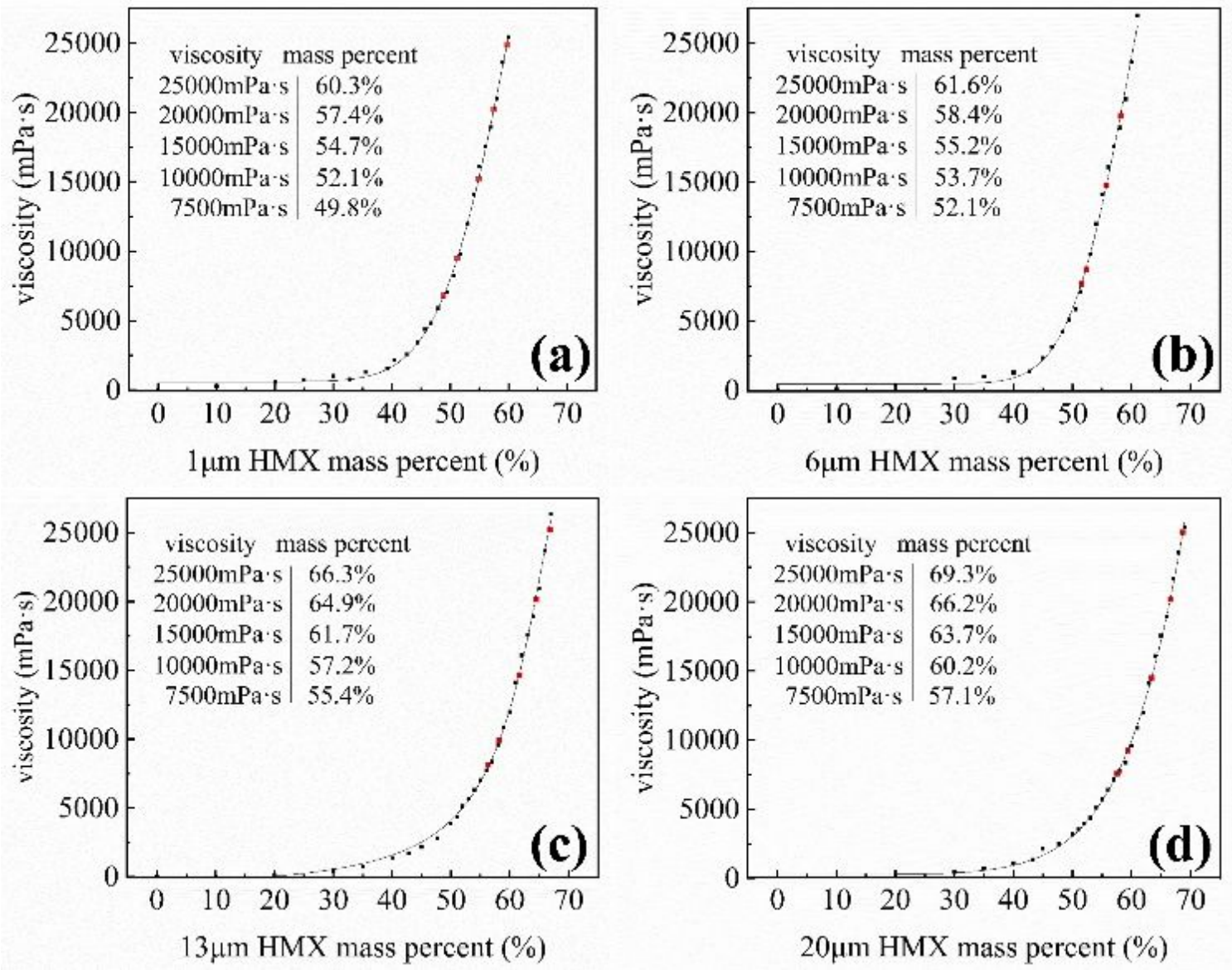

Figure 3

Effect of HMX contend and particle size on viscosity of molten TNT/HMX compositions.

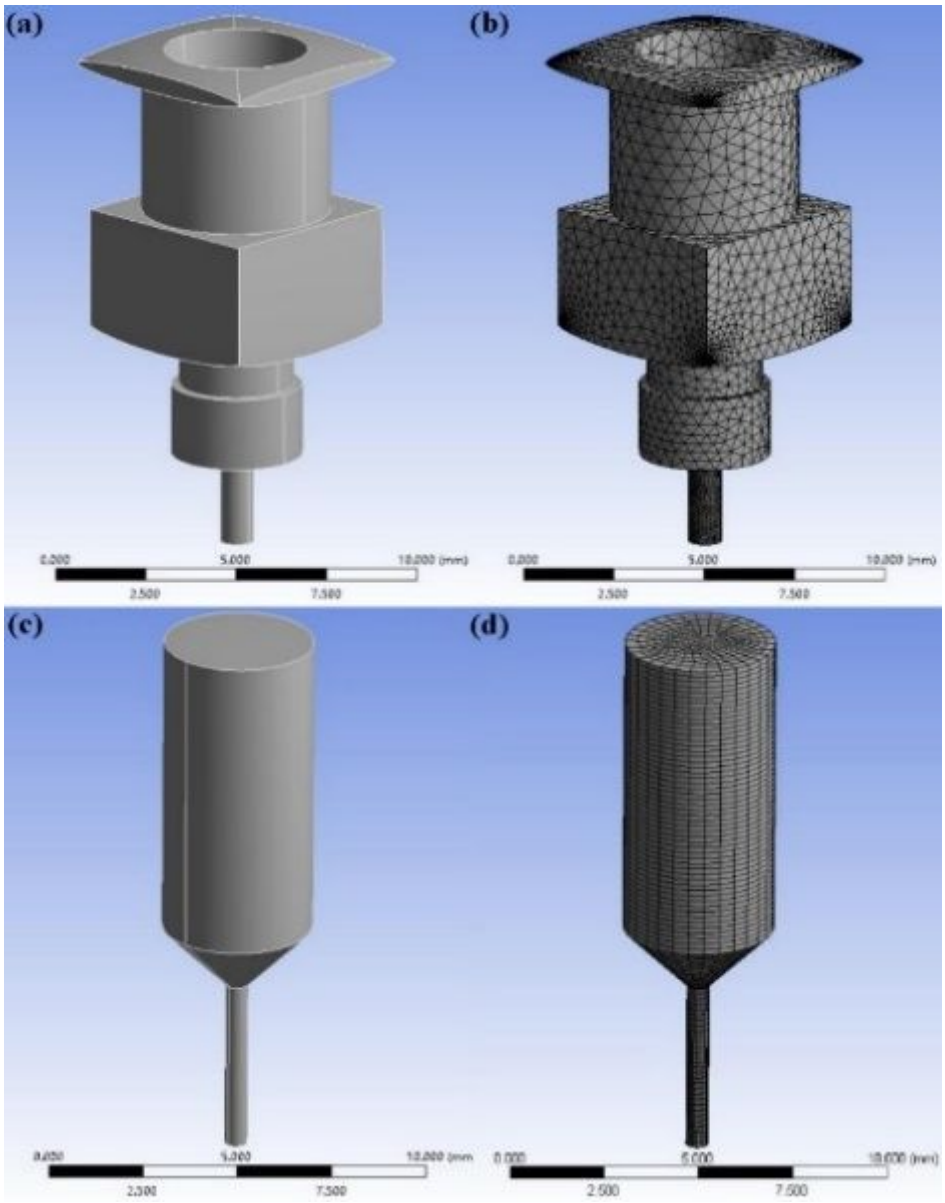

Figure 4

(a) 3D model of nozzle; (b) nozzle after meshed; (c) 3D model of flow channel; (d) flow channel after meshed.

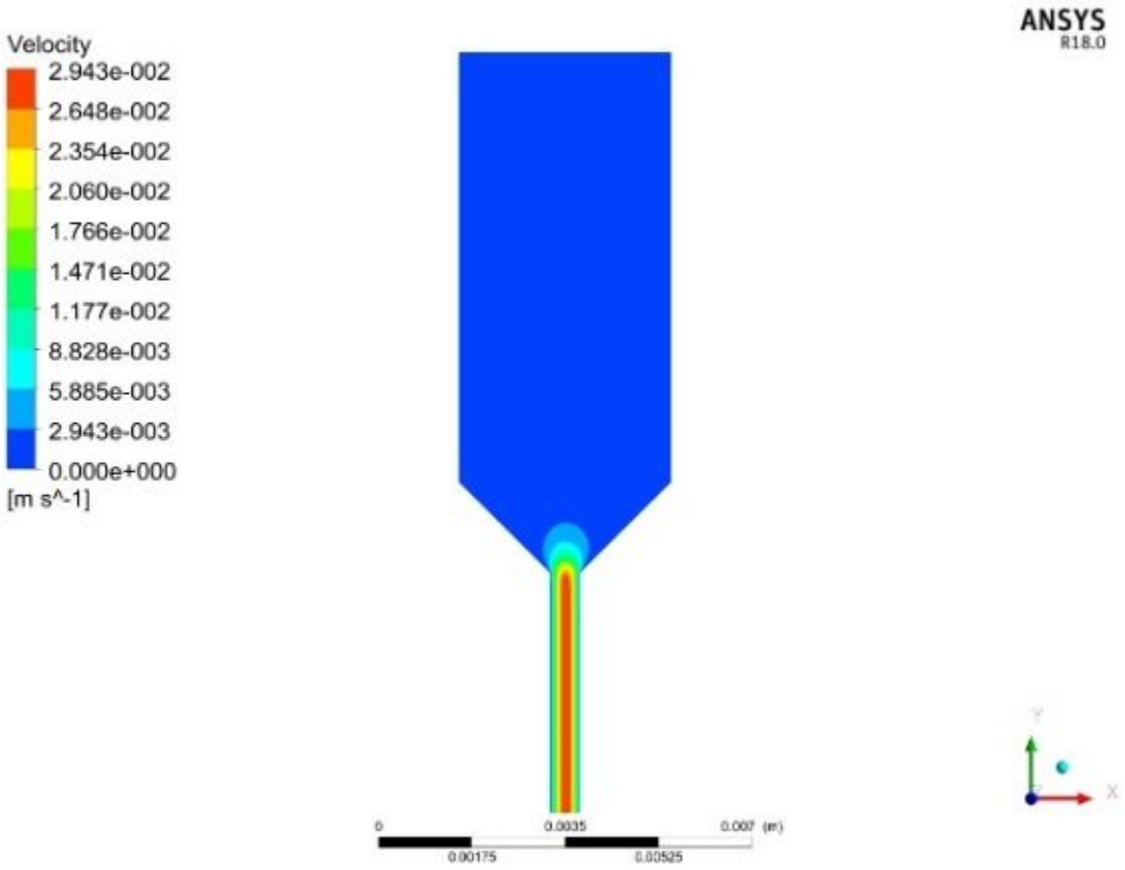

Figure 5

Velocity contour of the flow channel (25000 mPa•s).

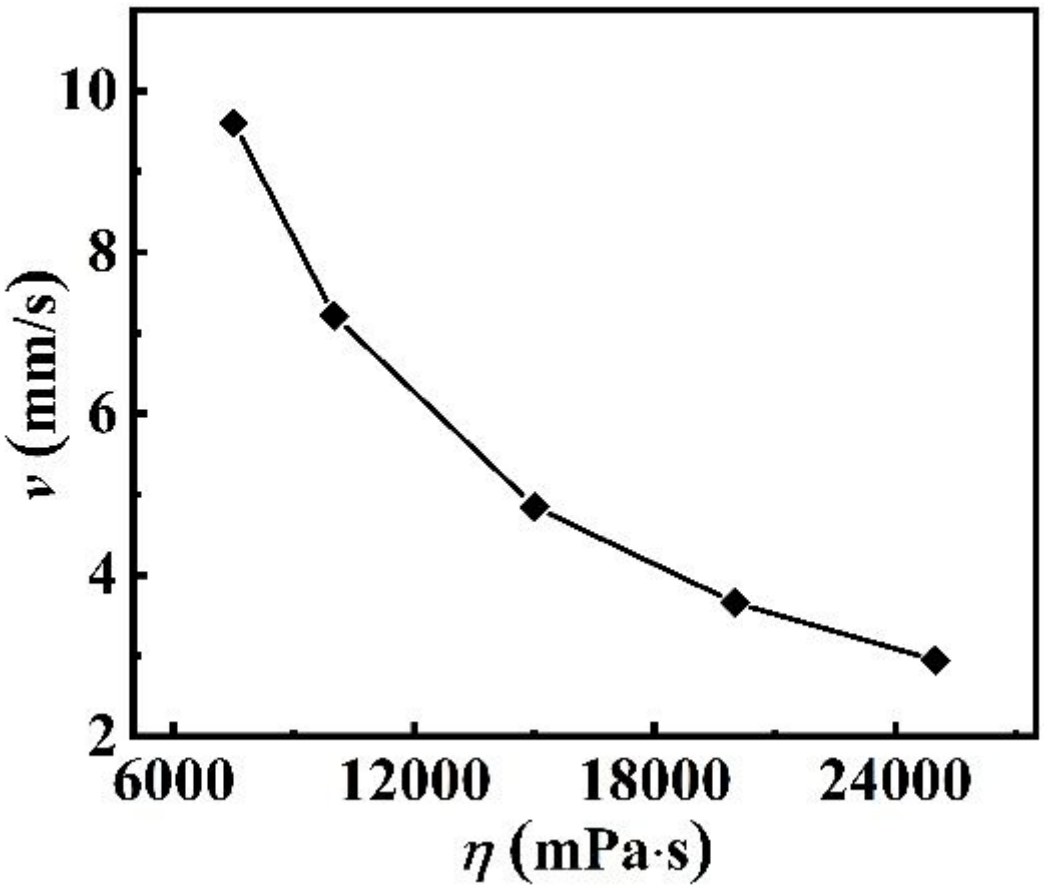

Figure 6

Velocity as the function of viscosity.

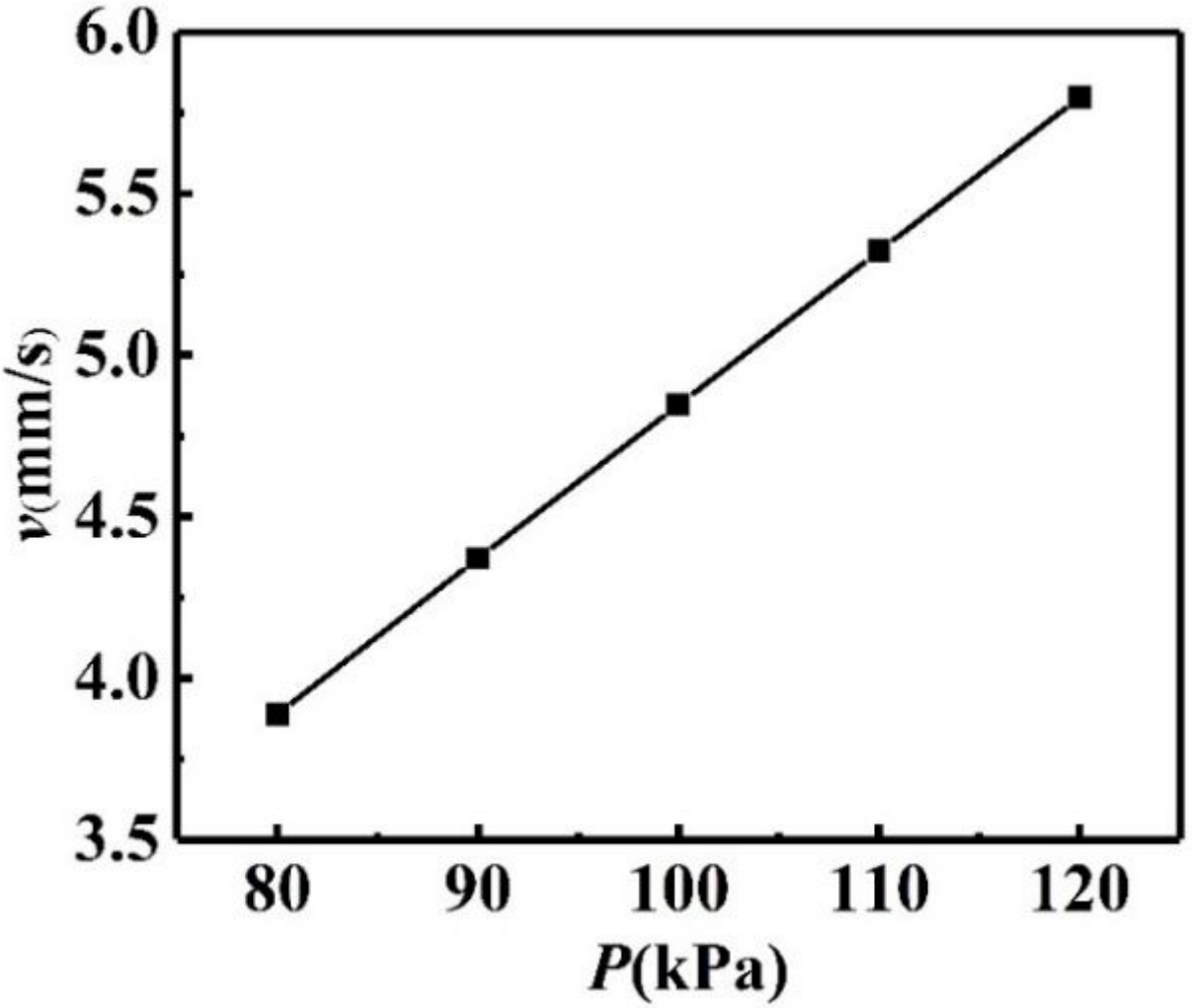

Figure 7

Velocity as the function of pressure.

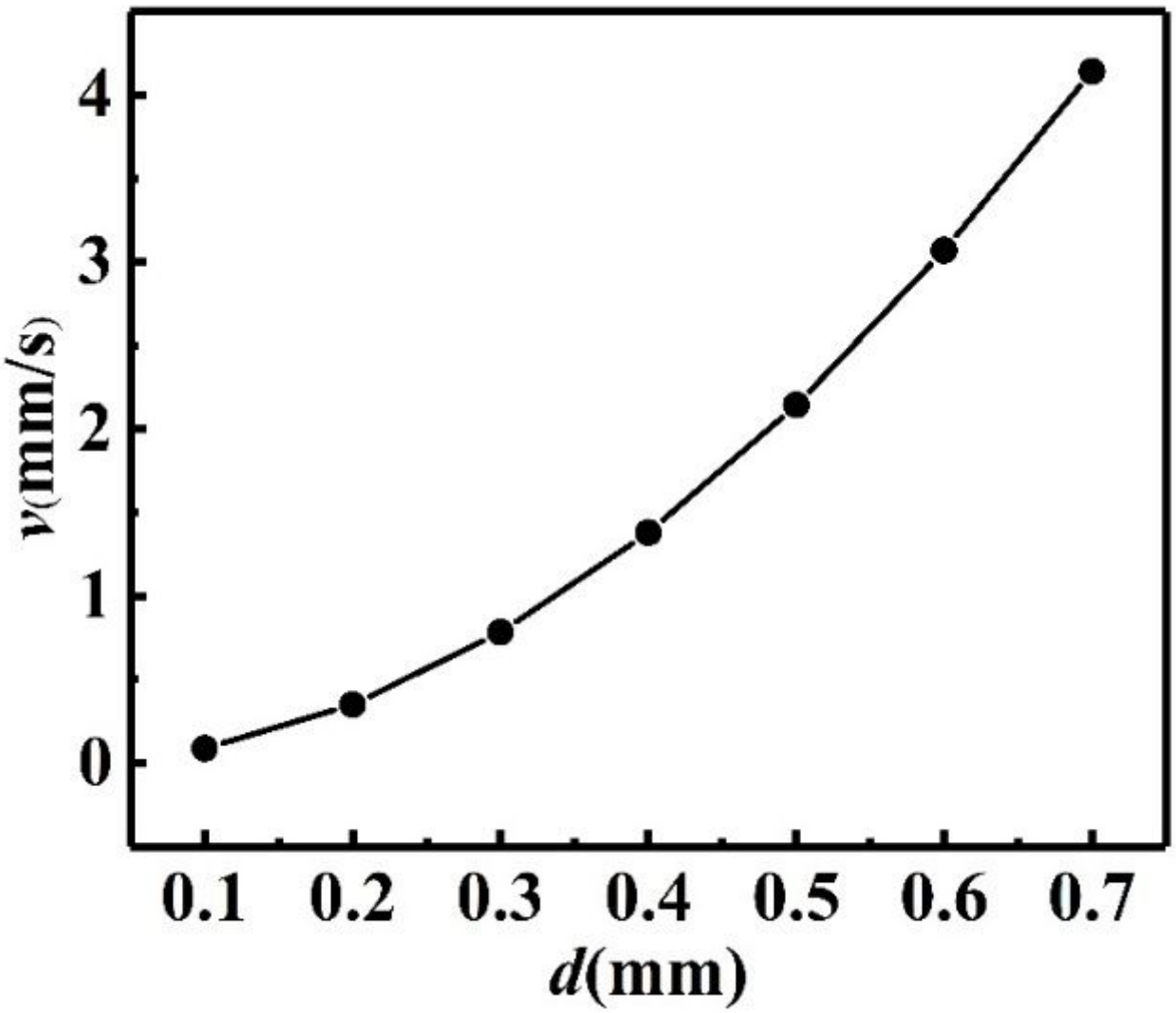

Figure 8

Velocity as the function of nozzle diameter.

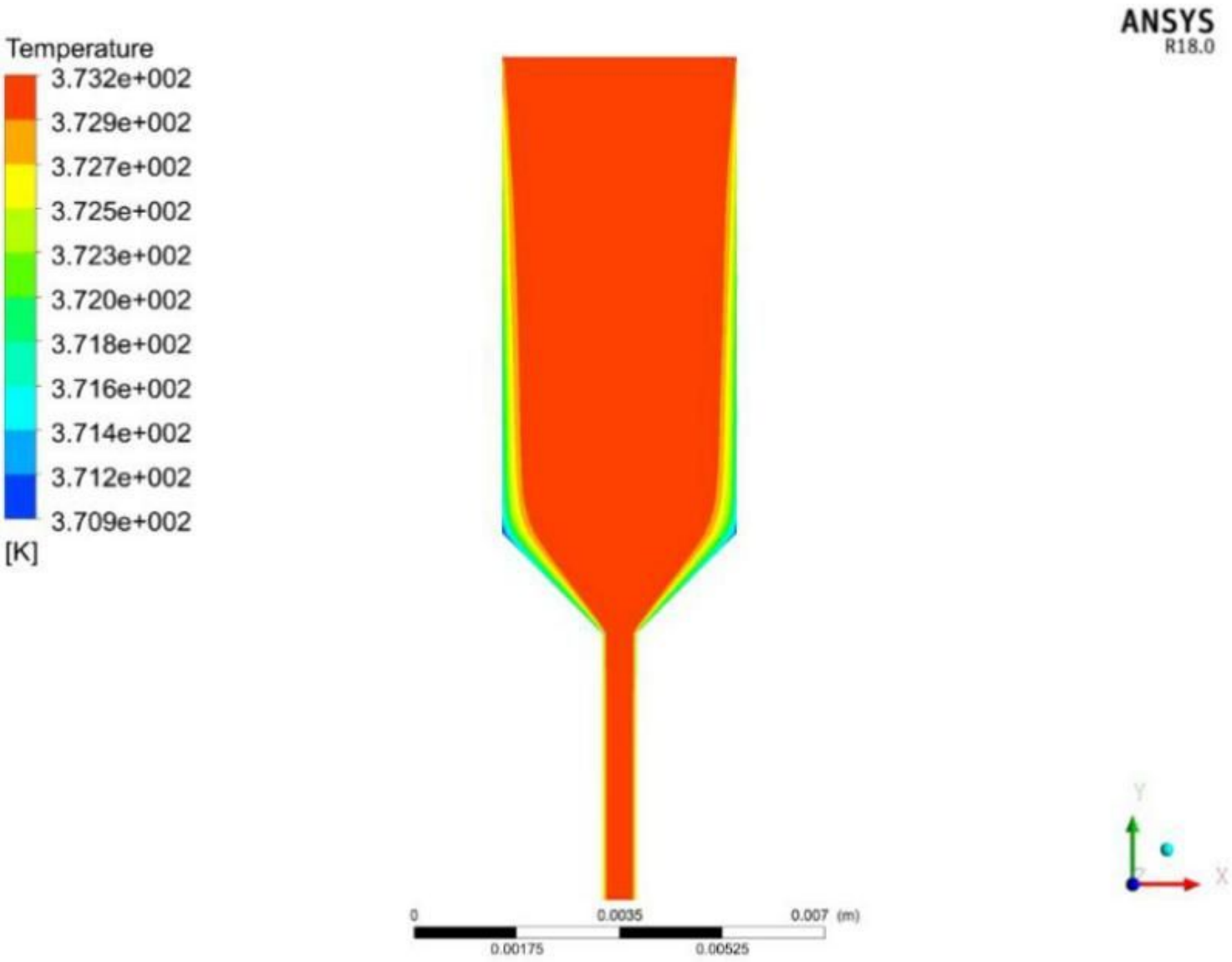

Figure 9

The temperature distribution of flow channel.

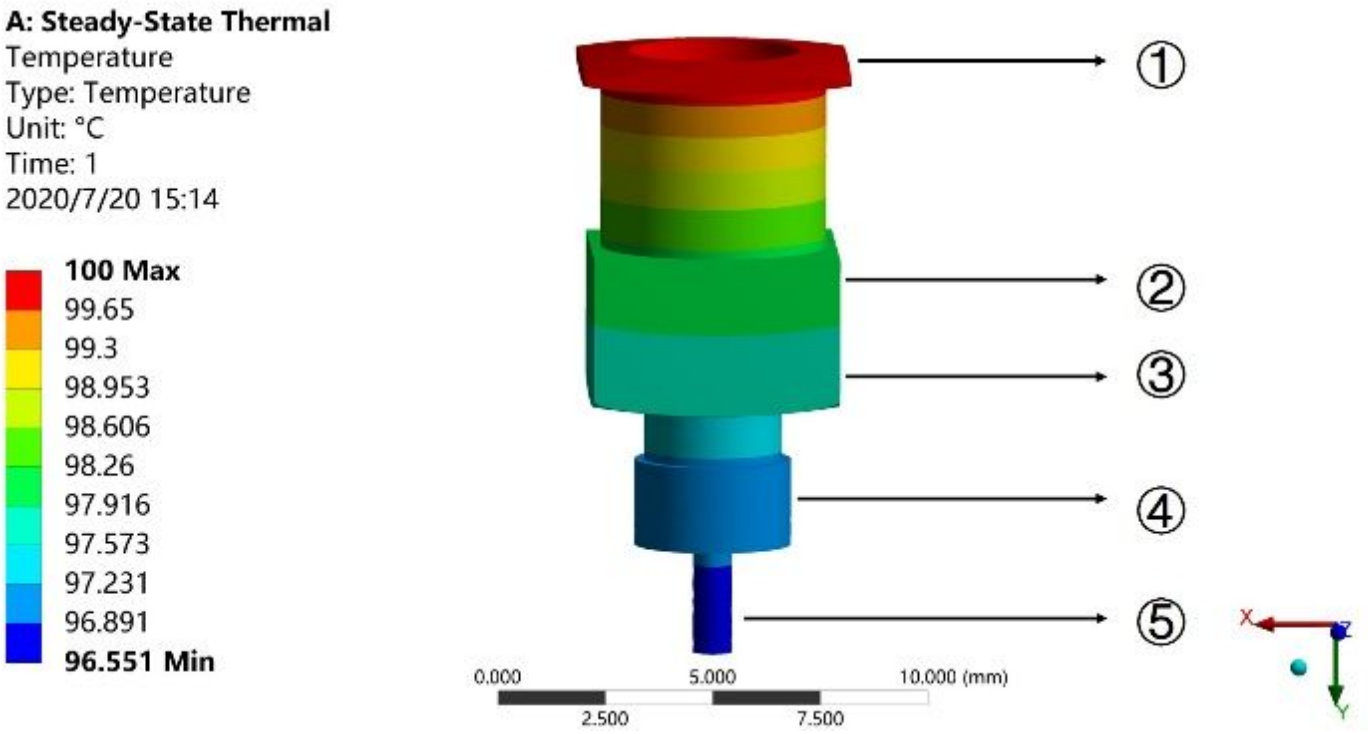

Figure 10

The temperature distribution of nozzle.

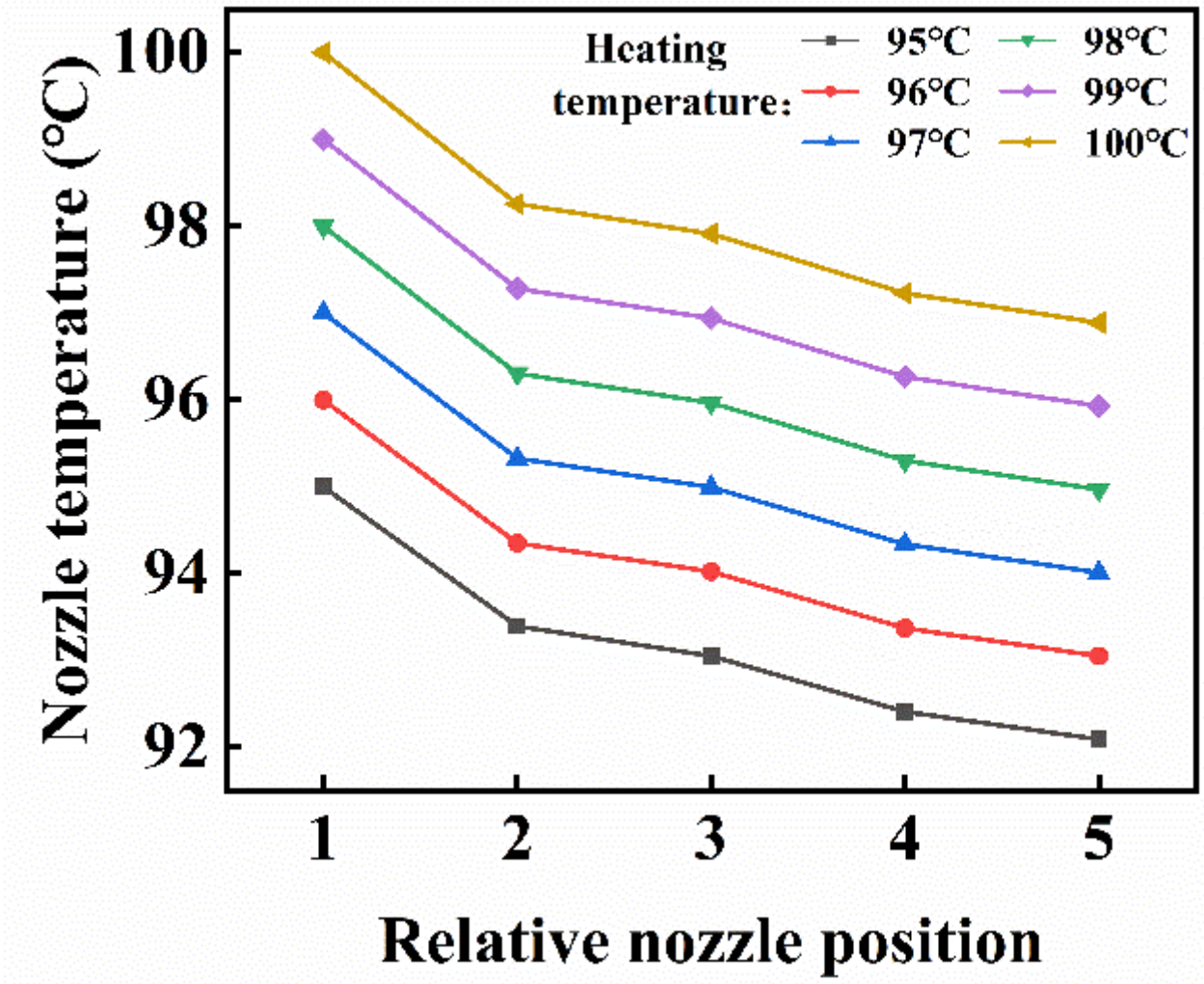

Figure 11

Temperature change with nozzle position

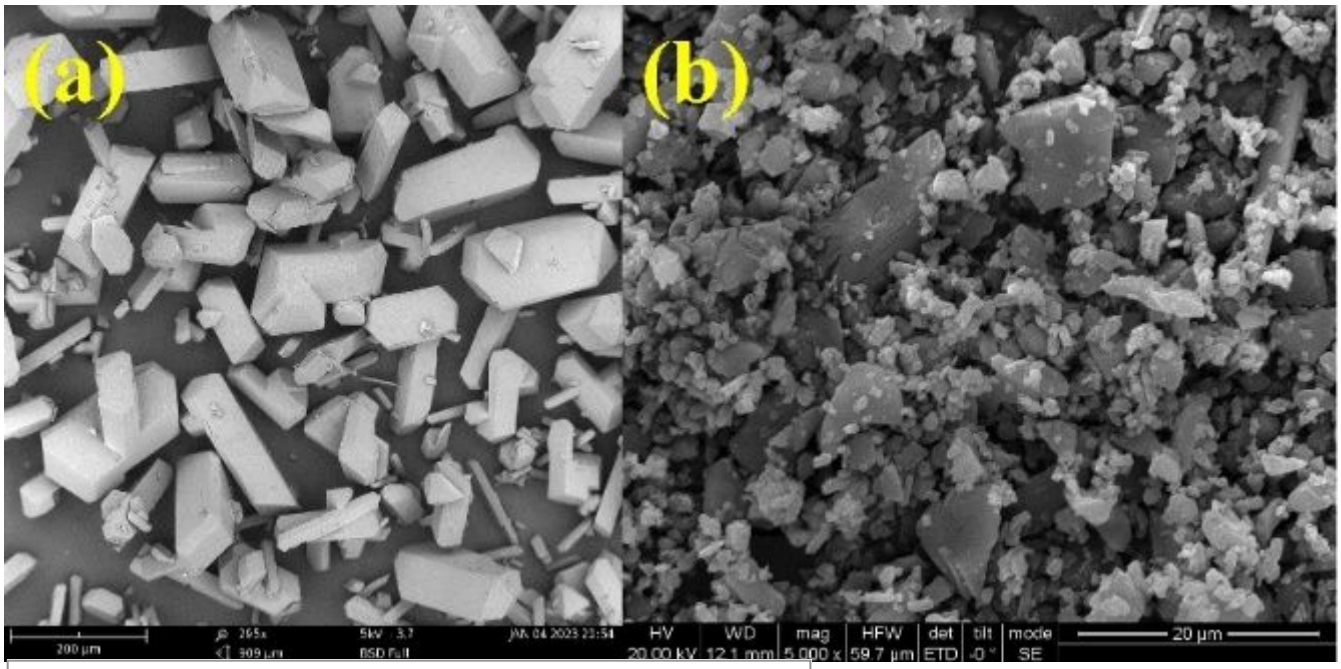

Figure 12

Raw HMX and milled HMX

Figure 13

The printer is printing the model

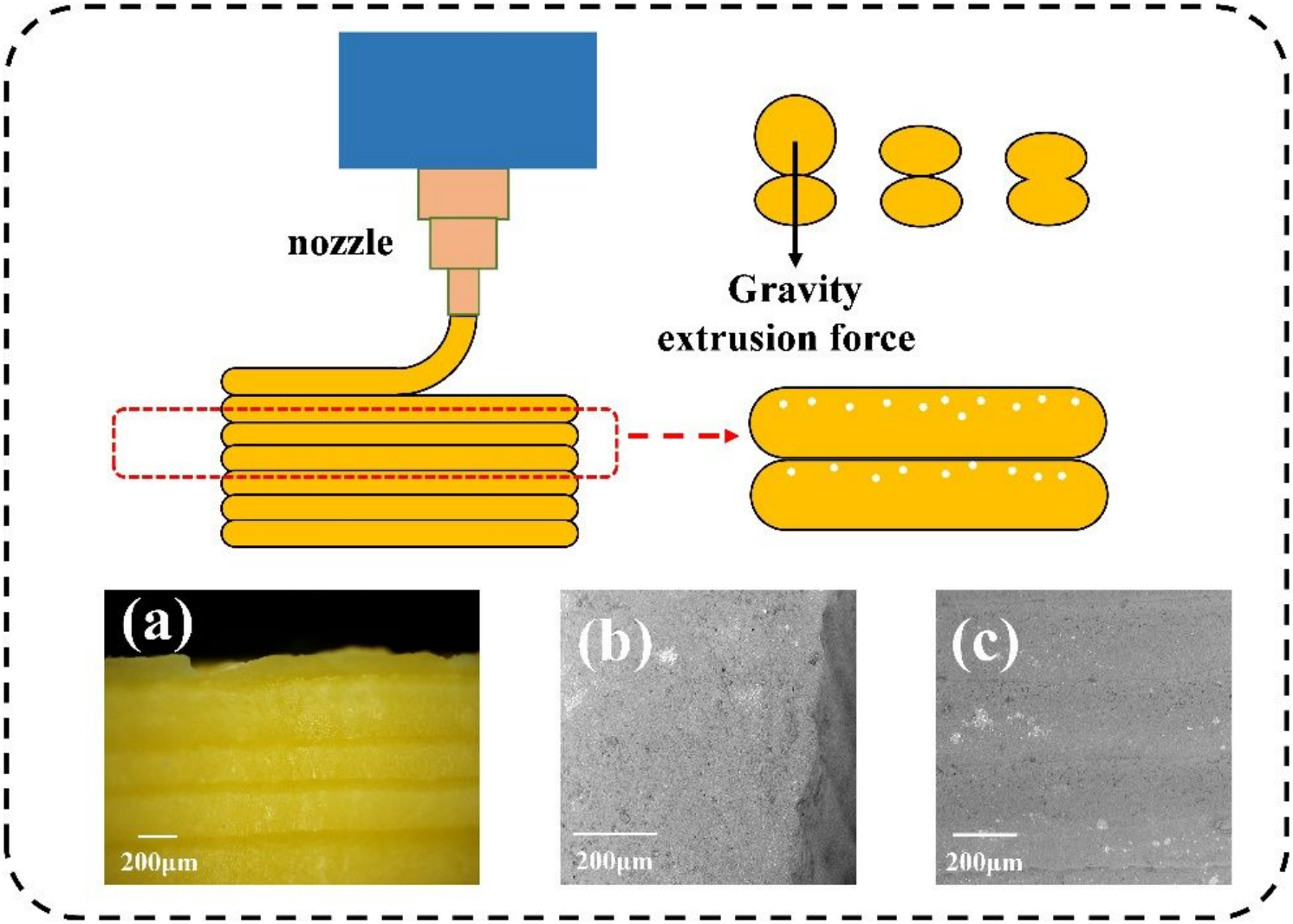

Figure 14

Flow chart of 3D printing HMX/TNT based explosives (a) Optical micrographs of 3D printed sample; SEM images of 3D printed sample (b)front view (c)sectional view

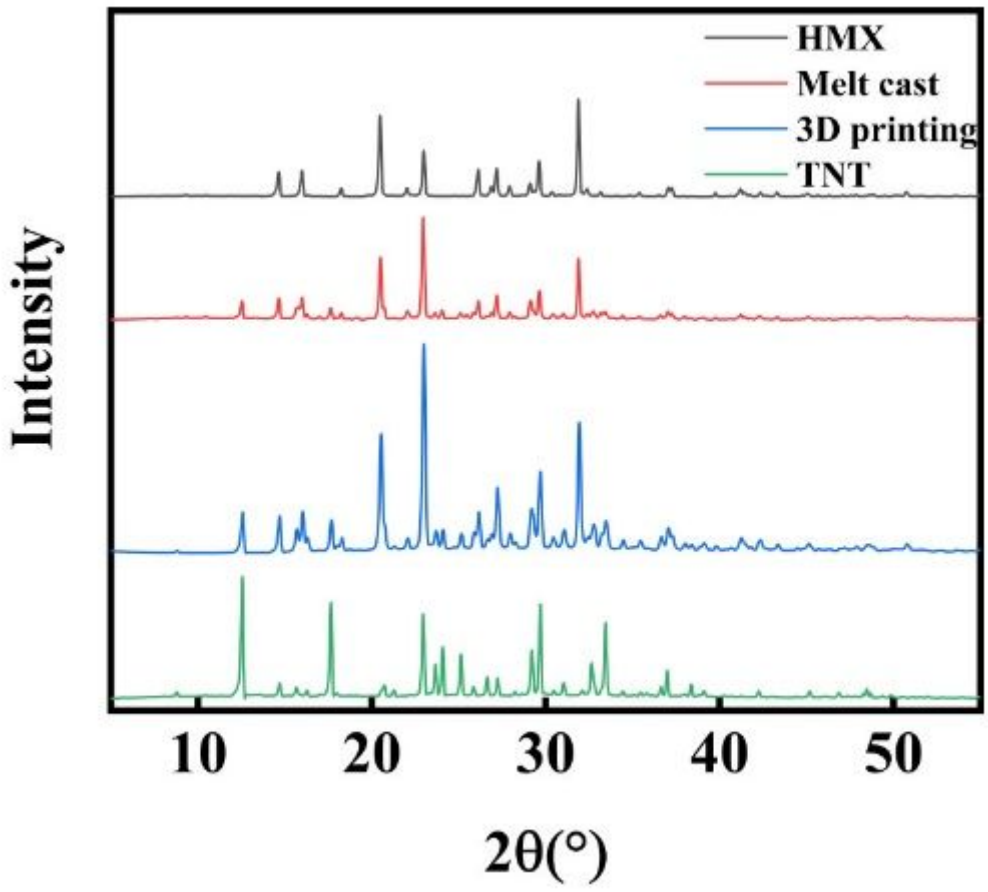

Figure 15

XRD pattern of HMX/TNT explosives prepared by melt cast and 3D printing